

Singlet and triplet polaron relaxation in doubly charged self-assembled quantum dots

T Grange^{1,6}, E A Zibik², R Ferreira¹, G Bastard¹, B A Carpenter², P J Phillips³, D Stehr⁴, S Winnerl⁴, M Helm⁴, M J Steer⁵, M Hopkinson⁵, J W Cockburn², M S Skolnick² and L R Wilson²

¹ Laboratoire Pierre Aigrain, Ecole Normale Supérieure, 24 rue Lhomond, 75231 Paris Cedex 05, France

² Department of Physics and Astronomy, University of Sheffield, Sheffield S3 7RH, UK

³ FOM Institute Rijnhuizen, PO Box 1207, NL-3430 BE, Nieuwegein, The Netherlands

⁴ Institute of Ion Beam Physics and Materials Research, Forschungszentrum Rossendorf, PO Box 510119, 01314 Dresden, Germany

⁵ EPSRC National Centre for III-V Technologies, Sheffield S1 3JD, UK

E-mail: thomas.grange@lpa.ens.fr, e.zibik@sheffield.ac.uk, robson.ferreira@lpa.ens.fr and luke.wilson@sheffield.ac.uk

New Journal of Physics **9** (2007) 259

Received 9 May 2007

Published 10 August 2007

Online at <http://www.njp.org/>

doi:10.1088/1367-2630/9/8/259

Abstract. Polaron relaxation in self-assembled InAs/GaAs quantum dot samples containing 2 electrons per dot is studied using far-infrared, time-resolved pump-probe measurements for transitions between the *s*-like ground and *p*-like first excited conduction band states. Spin-flip transitions between singlet and triplet states are observed experimentally in the decay of the absorption bleaching, which shows a clear biexponential dependence. The initial fast decay (~ 30 ps) is associated with the singlet polaron decay, while the decay component with the longer time constant (~ 5 ns) corresponds to the excited state triplet lifetime. The results are explained by considering the intrinsic Dresselhaus spin-orbit interaction, which induces spin-flip transitions by acoustic phonon emission or phonon anharmonicity. We have calculated the spin-flip decay times, and good agreement is obtained between the experiment and the simulation of the pump-probe signal. Our results demonstrate the importance of spin-mixing effects for intraband energy relaxation in InAs/GaAs quantum dots.

⁶ Author to whom any correspondence should be addressed.

Contents

1. Introduction	2
2. Theory	4
2.1. Energy spectrum of doubly charged QDs	4
2.2. Polaron relaxation	5
2.3. Spin-orbit interaction	6
2.4. Singlet to triplet spin-flip transition	7
2.5. Relaxation between triplet states	8
2.6. Spin triplet lifetime	8
3. Comparison of experiment and theory	8
4. Conclusion	11
Acknowledgments	11
Appendix. Triplet polaron calculation	11
References	12

1. Introduction

Carrier relaxation and dephasing processes in self-assembled quantum dots (QDs) have been major research areas in semiconductor physics in recent years. It was demonstrated both theoretically [1] and experimentally [2]–[4], that electrons confined in a self-assembled InAs/GaAs semiconductor QD strongly interact with the longitudinal optical (LO) vibrations of the crystal. This leads to the formation of QD polaron states. These states have been observed using intraband magneto-transmission experiments in the far-infrared (FIR) [2]–[5]. Polarons, however, are not stable entities, because of intrinsic anharmonic coupling which affects the LO-phonons [6, 7]. The decay of polarons from the first excited (p) state to the ground (s) state in the conduction band has been measured to be several tens of ps [8, 9]. This result brings an indisputable answer to the ‘phonon bottleneck’ issue in QDs, but also highlights the fact that excited QD states are affected by an important intrinsic, and thus unavoidable, source of dephasing.

To date, all polaron relaxation studies were performed on QD ensembles containing one electron per dot only. In the case of 2 electrons per dot ($2e/\text{dot}$), the polaron dynamics after FIR excitation to the p -state are more complicated due to possible electron spin-flip process and subsequent formation of the spin triplet state. Understanding the spin relaxation mechanisms in QD systems is very important for quantum information processing using the electron spin state. In [10] electron spin lifetimes up to 20 ms were measured between Zeeman-split spin levels of a InAs/GaAs QD in the presence of a magnetic field. In [11] it was shown that the spin state of the resident electron in an n -doped InAs/GaAs QD can be ‘written’ and ‘read’ using interband, circularly polarized optical pumping. In this case, the photoexcited and residual electrons can form a spin triplet, and the spin writing mechanism was explained by the interplay between periodic electron-hole flip-flops due to anisotropic exchange splitting and thermalization of the spin triplet. The lifetime of such triplet states, which plays a key role in the efficiency of the writing/reading process, is as yet unknown and is difficult to measure directly using conventional interband pump-probe or four-wave mixing experiments.

In this paper, we present the results of polaron relaxation and spin dynamic studies in *n*-doped self-assembled InAs/GaAs QDs using *intraband* pump–probe spectroscopy. Intraband experiments on 2e/dot samples enable study of singlet and triplet electron states without the presence of holes. The FIR radiation populates one excited singlet state and, as we show below, the relaxation back to the ground singlet state may either be due to a direct, spin-conserving process, or follow an indirect path involving two sequential spin–flip processes: one fast acoustic-phonon assisted transfer to lower energy triplet states, followed by a slow triplet-to-singlet relaxation by polaron disintegration (in ~ 5 ns, showing that the triplet lifetime is longer than the interband lifetime). This picture of the relaxation process is supported by our theoretical model, where we consider the Dresselhaus spin–orbit coupling together with electron–phonon interactions. Including the results of our calculation of the various spin–flip and spin-conserving decay times in a rate equation model yields good agreement with the experimentally observed polaron dynamics.

The InAs/GaAs QD samples studied were grown on (100) GaAs substrates by molecular beam epitaxy in the Stranski–Krastanow mode. The structures contain 80 layers of InAs QDs separated by 50 nm intrinsic GaAs spacers. Prior to growth of the multilayer samples, an uncapped reference sample was grown from which we were able to determine the QD density ($\sim 4 \times 10^{10} \text{ cm}^{-2}$) from atomic force microscope analysis. In order to achieve the dot population of either 1 (sample A) or 2e/dot (samples B and C), the QD structures were modulation doped with a Si concentration of $4 \times 10^{10} \text{ cm}^{-2}$ or $8 \times 10^{10} \text{ cm}^{-2}$, respectively with the doping layer 2 nm below the wetting layer. In order to confirm that the QDs in the 2e/dot samples (B and C) contain 2 electrons photoluminescence excitation (PLE) measurements were carried out. For these samples, absorption into the conduction band ground state should be blocked as it is fully occupied. It was observed that the sample with one electron per dot exhibits a peak at ~ 36 meV above the detection energy, corresponding to the ground state LO-phonon replica, whereas the samples doped to contain 2e/dot have no such feature. This result shows that the interband absorption between electron and hole ground states with the involvement of LO-phonons is blocked, indicating that for the 2e/dot samples the electron ground state is indeed fully occupied. In addition, the 1e/dot and 2e/dot samples were studied using the FIR magneto-transmission measurements [5] and a clear increase of the electron–phonon coupling strength was experimentally observed for the 2e/dot sample, the origin of which will be discussed later in section 2.2.

The relaxation dynamics of excited polarons in QDs were studied using degenerate FIR pump–probe spectroscopy [12]. Polaron transitions between the *s*-like ground state and *p*-like first excited states have an in-plane dipole and therefore, can be observed in normal incidence geometry. The Dutch free electron laser (FELIX) was used to provide picosecond pulses polarized along the [0 $\bar{1}$ 1] crystallographic direction and tuned into resonance with optical transitions between the *s*-state and the lower energy *p*-like state, p_x [9, 13]. The low temperature pump–probe signal measured at the same excitation energy of ~ 55 meV for the 1 and 2e/dot samples is shown in figure 1. There is a clear difference in the time evolution of the absorption bleaching. The 1e/dot sample exhibits a mono-exponential decay of the pump–probe signal with a time constant of $\tau_1 = 50 \pm 4$ ps, whereas the 2e/dot sample has a bi-exponential dependence with a short time decay of 30 ± 3 ps and a long time component decaying on a nanosecond timescale [13].

The intraband relaxation for 1e/dot samples has been studied in detail in our previous work [9] with the observed decay arising from the intrinsic instability of QD polaron states [6].

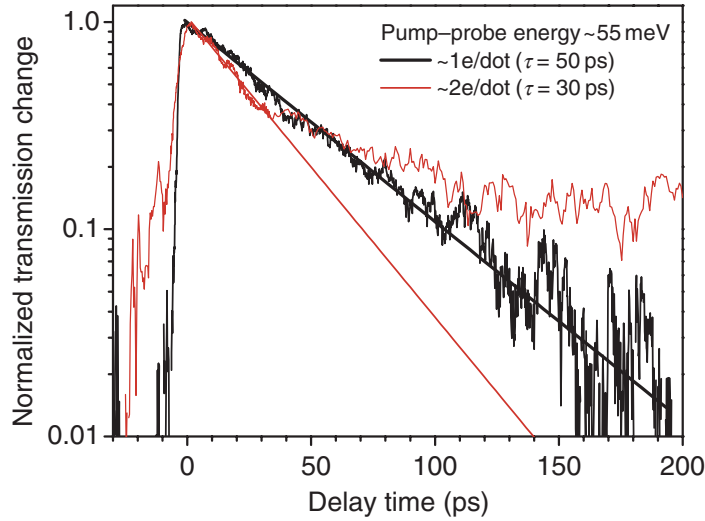


Figure 1. Normalized 5 K transmission change as a function of time delay between the pump and probe at energy of 55 meV for 1 (A) and 2e/dot (B) samples (thick black and thin red lines respectively). The mono-exponential fits used to extract the decay times are also shown.

We show here that the biexponential behaviour for 2e/dot samples is related to scattering processes among admixed singlet and triplet QD polarons. The latter results from three principal couplings for the confined electrons: (i) their direct and exchange (Coulomb) interactions, responsible for the formation of singlet and triplet states, (ii) the electron–LO phonon (Fröhlich) coupling, which leads to the formation of two-electron polaron states, and (iii) the spin–orbit (Dresselhaus) coupling due to the non-parabolic band structures of the host materials, which mixes singlet and triplet states.

2. Theory

2.1. Energy spectrum of doubly charged QDs

The 2 electron singlet and triplet states of the QD are calculated by diagonalizing the direct and exchange Coulomb interactions within a truncated basis of the first three bound electron orbitals: s , p_x and p_y . The electronic levels are calculated using a one-band model for a $\text{Ga}_x\text{In}_{1-x}\text{As}$ QD. The dot is modeled by a truncated cone with a circular base. Dot size and mole fraction $x = 0.4$ are chosen to match simultaneously the interband (1.12 eV) and intraband (55 meV) energies respectively measured in PL and used in pump–probe experiments. Anisotropy splitting of $2V_A$ between the p_y and p_x levels is included from the experiment. This anisotropy can be explained by elongation of the QDs along the in-plane $[0\bar{1}1]$ direction [14], piezoelectric field effects [15] and the atomistic symmetry [16].

The scheme of the low-lying two-electron states is presented in figure 2 (the superscript S and T refer to singlet and triplet respectively). In this figure, V_E is the Coulomb exchange energy:

$$V_E = \langle s^{(1)} p_u^{(2)} | \frac{e^2}{4\pi \epsilon_0 \epsilon_r |r^{(1)} - r^{(2)}|} | p_u^{(1)} s^{(2)} \rangle, \quad (1)$$

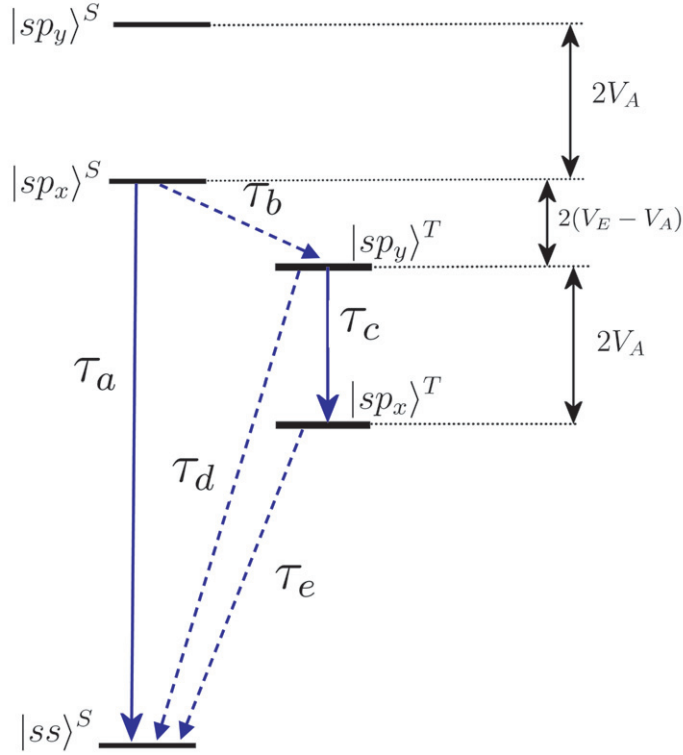


Figure 2. Energy diagram of quantum dots charged with 2 electrons. Singlet and triplet states appear respectively on the left and right side, with superscript S and T respectively. The solid and dashed arrows represent respectively spin-conserving and spin-flip relaxation channels.

where $u = x$ or y and superscripts label each of the 2 electrons. Taking the dielectric constant as $\epsilon_r = 14.3$, we calculate $2V_E = 10.5$ meV (see, for example, [17] for measurements of V_E). For typical QDs, $2V_A$ is smaller than $2V_E$, and both the $|sp_x\rangle^T$ and $|sp_y\rangle^T$ sets of triplet states have lower energies than the first excited singlet state $|sp_x\rangle^S$. In this figure, solid and dashed arrows indicate the different spin-conserving (τ_a , τ_c) and spin-flip (τ_b , τ_d , τ_e) relaxation processes that can occur after the photo-excitation of the first excited singlet state $|sp_x\rangle^S$.

2.2. Polaron relaxation

Coupling of electrons to LO-phonons generates spin-diagonal singlet and triplet polaron states. The polaron wavefunctions are entanglements of decoupled states $|(ab)^L, n\rangle$ where $a, b = s, p_x$ or p_y , $L = S$ or T and n is the number of LO-phonon modes entering in the formation of the polaron (see, for example [4]). The matrix element at the origin of the polaron for the two electron case is $\sqrt{2}$ stronger for the singlet as compared to the one-electron case:

$$\langle (ss)^S, 1 | H_F^{(1)} + H_F^{(2)} | (sp_x)^S, 0 \rangle = \sqrt{2} \langle s, 1 | H_F | p_x, 0 \rangle, \quad (2)$$

where H_F is the Fröhlich Hamiltonian. In [5], this increase of the electron-phonon coupling strength was experimentally demonstrated for the sample B using intraband magneto-transmission experiments. Since the coupling strength (~ 7 meV) is much smaller than the

energy detuning (19 meV) between the two interacting states (the energy of center-zone LO-phonons is taken as $E_{\text{LO}} = 36$ meV), the schematic diagram in figure 2 also holds for polaron states with dominant 0-phonon components. As a consequence of equation (2), the singlet polaron has a LO-phonon weight almost twice as large and thus an anharmonic lifetime (τ_a) roughly two times (the ratio is 1.9 in the exact calculation) shorter than the corresponding 1e/dot polaron probed with the same photon energy. In figure 1, we measure a decay time of $\tau_a \simeq 30$ ps, close to the predicted value of $\tau_1/1.9 \simeq 26$ ps. Apart from uncertainty of the measurements, the small discrepancy may arise from doping uncertainty of the QD ensemble (a small fraction of dots in the 2e/dot sample might also contain 1 electron [18]).

2.3. Spin-orbit interaction

Exchange of population between the photo-excited singlet state and the lower energy triplet states can be calculated by considering the Dresselhaus interaction [19], which is an intrinsic spin-orbit coupling mechanism in crystals without inversion symmetry. The bulk Dresselhaus Hamiltonian reads:

$$H_D = \gamma \boldsymbol{\sigma} \cdot \boldsymbol{\kappa}, \quad (3)$$

where $\boldsymbol{\sigma}$ are the Pauli matrices, $\kappa_x = k_x(k_y^2 - k_z^2)$, $\kappa_y = k_y(k_z^2 - k_x^2)$, $\kappa_z = k_z(k_x^2 - k_y^2)$ with $\mathbf{k} = -i\nabla$ the electron wavevector operator, and γ a material-dependent constant: $\gamma_{\text{GaAs}} = 7$ au and $\gamma_{\text{InAs}} = 26$ au [20, 21]. In the 1e/dot case, s - and p -states with opposite spins are coupled by $V_{\text{sp}}^D = \gamma \langle s | \kappa_x | p_x \rangle$. For $\gamma = 22$ au (this value is discussed below), we calculate $|V_{\text{sp}}^D| = 3.9$ meV. Note that we have numerically checked that the Rashba spin-orbit coupling [22] between these states is negligible in our QDs: it is two orders of magnitude weaker than V_{sp}^D . For 2e/dot, the Dresselhaus Hamiltonian couples singlet and triplet states. There are two spin-orbit interactions involved in the spin-flip mechanisms. Firstly, the $|sp_x\rangle^S$ singlet state is coupled to the two $|p_x p_y\rangle_{\pm 1}^T$ triplet states (not shown in figure 2) by:

$$\langle (sp_x)^S | H_D^{(1)} + H_D^{(2)} | (p_x p_y)_{\pm 1}^T \rangle = -\frac{V_{\text{sp}}^D}{\sqrt{2}}, \quad (4)$$

where for triplet states, subscript 0, ± 1 indicate total spin projection along the QD growth (z) axis. After diagonalization, the singlet wavefunction becomes an admixture of singlet and triplet, and reads in first-order perturbation theory:

$$\widetilde{|sp_x\rangle^S} \simeq |sp_x\rangle^S - \frac{V_{\text{sp}}^D}{\sqrt{2}E_{\text{sp}}} (|p_x p_y\rangle_{-1}^T + |p_x p_y\rangle_{+1}^T), \quad (5)$$

where E_{sp} is the one-electron s - p energy transition. Secondly, the $|ss\rangle^S$ ground state is coupled to the two $|sp_{x/y}\rangle_{\pm 1}^T$ triplet states by:

$$\langle (ss)^S | H_D^{(1)} + H_D^{(2)} | (sp_{x/y})_{\pm 1}^T \rangle = -V_{\text{sp}}^D. \quad (6)$$

The eigenstate with dominant triplet component therefore reads:

$$\widetilde{|sp_{y/x}\rangle_{\pm 1}^T} \simeq |sp_{y/x}\rangle_{\pm 1}^T + \frac{V_{\text{sp}}^D}{E_{\text{sp}}} |ss\rangle^S. \quad (7)$$

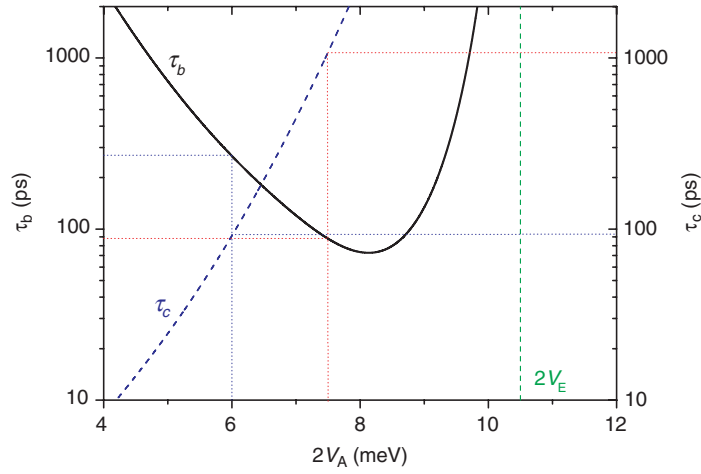


Figure 3. Singlet to triplet spin–flip time τ_b (solid line) and triplet to triplet decay time τ_c (dashed line) as a function of the anisotropy splitting ($2V_A$) at $T = 0$ K. Dotted lines indicate calculated values corresponding to anisotropy splitting measurements on the 2 studied samples.

2.4. Singlet to triplet spin–flip transition

Due to spin-mixing described above, relaxation by emission of longitudinal acoustic (LA) phonons between the eigenstates described by equations (5) and (7) is allowed. The relaxation time τ_b is given by:

$$\begin{aligned} \frac{1}{\tau_b} &= \frac{2\pi}{\hbar} \sum_{i=-1}^1 \sum_{\mathbf{q}} \left| \langle (sp_x)^S, n_{\mathbf{q}} | H_a | (sp_y)^T, (n+1)_{\mathbf{q}} \rangle \right|^2 \delta(\epsilon_{\mathbf{q}} - 2(V_e - V_a)) \\ &\simeq 2 \left(\sqrt{2} + \frac{1}{\sqrt{2}} \right)^2 \left(\frac{V_{sp}^D}{E_{sp}} \right)^2 \sum_{\mathbf{q}} \left| \langle p_x, n_{\mathbf{q}} | H_a | s, (n+1)_{\mathbf{q}} \rangle \right|^2 \delta(\epsilon_{\mathbf{q}} - 2(V_e - V_a)), \end{aligned} \quad (8)$$

where H_a is the deformation potential Hamiltonian for acoustic phonons, and $n_{\mathbf{q}}$ is the Bose occupation number for LA-phonons of wavevector \mathbf{q} . The factor 2 takes into account the relaxation towards the two different triplet states ± 1 . In figure 3, this spin flip time is calculated at low temperature as a function of the anisotropy splitting $2V_A$.

Note that this spin–flip time is a minimum when the energy separation $2(V_E - V_A)$ (the $|sp_x\rangle^S - |sp_y\rangle^T$ splitting) corresponds approximately to a phonon wavelength of the dot size. For the samples studied below, $2(V_E - V_A)$ values are typically a few meV, leading to spin–flip times of hundreds of picoseconds. Energy relaxation triggered by hyperfine interaction [23] with nuclear spins can be neglected for the meV energy changes considered here. The additional relaxation from the $|sp_x\rangle^S$ singlet toward the lower triplet states $|sp_x\rangle^T$ is given by the same calculation, except that the energy of the emitted phonon is $2V_E = 10.5$ meV, so that this relaxation channel can be safely neglected.

2.5. Relaxation between triplet states

Once in the upper triplet state $|sp_y\rangle^T$, a spin-conserving transition assisted by acoustic phonon emission occurs toward the lower set of triplet states $|sp_x\rangle^T$. Calculation of this decay time (τ_c) as a function of the anisotropy splitting is shown by dashed line in figure 3. Note that this time is equal to the decay time from p_y to p_x in the one-electron case, which has been studied in [9]. Calculated values of τ_c are 95 ps and 1.1 ns for $2V_A = 6.0$ and 7.5 meV respectively.

2.6. Spin triplet lifetime

The relaxation paths *d* and *e* involve spin mixing as well as polaron decay. First we diagonalize Fröhlich interactions between different LO-phonon states, the corresponding eigenvalues being polaron states: the lower triplet polaron states are $|(sp_{y/x})_{\pm 1}^T, \tilde{0}_{sp}\rangle$, while the singlet polaron ground state is $|ss, \tilde{0}_{ss}\rangle$ and its one-phonon replicas are $|ss, \tilde{1}_{ss}(q)\rangle$ (see appendix for definition and properties of the LO-phonon modes introduced here).

As we have seen in equation (6), the spin-orbit interaction couples the $|sp\rangle_{\pm 1}^T$ and $|ss\rangle^S$ electronic states. Taking this spin-orbit coupling in perturbation within the polaron basis introduced above, one obtains the spin-admixed polaron states with dominant zero-phonon triplet component:

$$|\widetilde{(sp_{y/x})_{\pm 1}^T}\rangle \simeq |(sp_{y/x})_{\pm 1}^T, \tilde{0}_{sp}\rangle + \frac{V_{sp}^D}{E_{d/e}} \langle \tilde{0}_{ss} | \tilde{0}_{sp} \rangle |ss, \tilde{0}_{ss}\rangle + \frac{V_{sp}^D}{E_{d/e} - E_{LO}} \sum_q \langle \tilde{1}_{ss}(q) | \tilde{0}_{sp} \rangle |ss, \tilde{1}_{ss}(q)\rangle \quad (9)$$

where $E_{d/e}$ is the energy separation corresponding to transitions *d* and *e*, respectively. The lifetimes of these polarons, due to anharmonicity of their LO-phonon component, reads:

$$\frac{1}{\tau_{d/e}} = \frac{1}{\tau_{LO}(E_{d/e})} \left| \frac{V_{sp}^D}{E_{d/e} - E_{LO}} \right|^2 \sum_q \left| \langle \tilde{1}_{ss}(q) | \tilde{0}_{sp} \rangle \right|^2 \quad (10)$$

where τ_{LO} is the decay time of center-zone LO phonons into two acoustic phonons of total energy $E_{d/e}$, which is extracted from polaron studies of 1e/dot samples [9, 24]. We calculate $\tau_e = 4.9$ ns, while $\tau_d = 10$ and 12 ns for respectively $2V_A = 6.0$ and 7.5 meV.

3. Comparison of experiment and theory

Here, we focus on the long decay time behavior and its temperature dependence for the two QD samples doped to contain 2e/dot (B and C) measured on a longer timescale compared to figure 1 using the free electron laser FELBE⁷. The pump-probe signal for the samples B and C is presented in figure 4(a). The anisotropic splitting V_A was determined from the FIR linear absorption spectra measured in normal incidence geometry at 5 K, which are shown in the figure 4(a) inset. Incident radiation polarized along the $[0\bar{1}1]$ ($[011]$) crystallographic direction excites a transition from the *s*-like ground state to the lower (higher) energy laterally confined *p*-like excited state. The absorption peaks associated with transitions to the lower energy *p*-like

⁷ The experimental conditions with the FELBE set-up were not optimized for measurements of the short decay time component, in particular an accurate measurement is hindered by back reflection of the pump beam inside the sample resulting in additional peak in the pump-probe decay curve at ~ 10 ps.

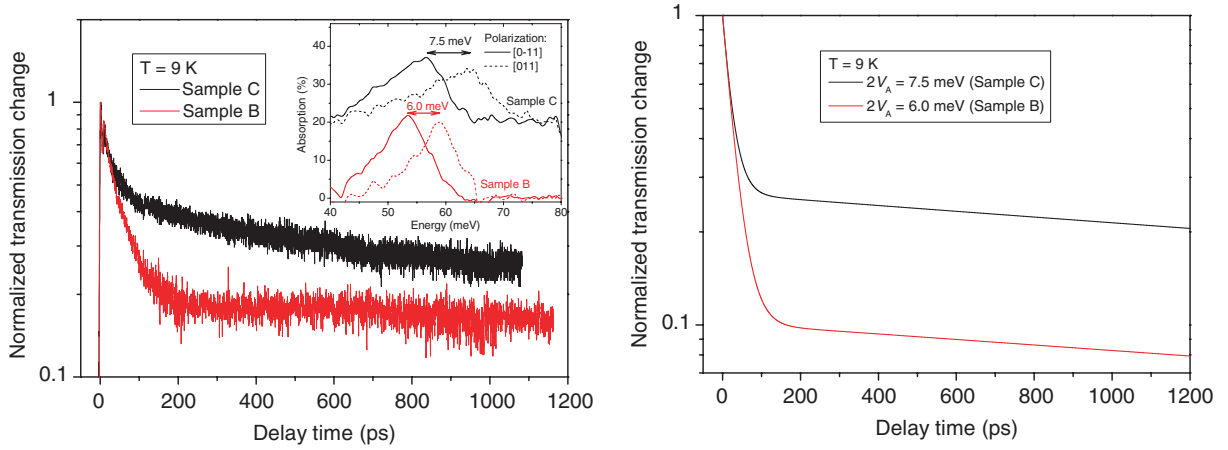


Figure 4. (a) Measured time evolution of the s - p transmission change for polarons formed by 2-electrons for sample B (red line) and sample C (black line). Inset: normal incidence absorption spectrum for incident radiation polarized along $[0\bar{1}1]$ (solid line) and $[011]$ (dashed line) for samples B (red line) and sample C (black line, vertically offset by 20% for clarity). (b) Calculated pump-probe dynamics for anisotropic splitting of 6.0 meV (red line) and 7.5 meV (black line).

state (p_x) and higher energy p -like state (p_y) are centered at 53 and 58 meV, respectively, for the sample B. The sample B has an anisotropic splitting $2V_A$ of ~ 6.0 meV whilst sample C splitting is $2V_A \sim 7.5$ meV. The increase of the p -state splitting for the sample C is probably due to slightly larger QD asymmetry in the lateral direction for this sample.

The two samples exhibit biexponential absorption recovery with long decay times of ~ 2 and ~ 5 ns for C and B samples, respectively⁸. We present in figure 4(b) the calculation of the population recovery of the ground state after population at $t = 0$ of the first excited singlet state, accounting for the different spin-conserving and spin-flip energy relaxation paths indicated on figure 2. The set of linear rate equations incorporating the various scattering processes that occur within the five level system in figure 2 were solved numerically. The normalized transmission change was taken equal to $1 - N_g$, where the ground state population verified $N_g = 0$ after laser pump ($t = 0$) while the population of the photo-excited $|sp_x^s\rangle$ state was set to 1. In this simulation, $\tau_a = 30$ ps was extracted from the fit of figure 1, while τ_b , τ_c , τ_d and τ_e were calculated as described above, for the two different experimental values of $2V_A$: 6.0 and 7.5 meV (all other parameters being the same). The calculations are made with $\gamma = 22$ au, which corresponds to the best agreement between calculated and measured triplet lifetime of ~ 5 ns for sample B. Note that the simulation is very sensitive to γ , since τ_b and τ_e are proportional to $1/\gamma^2$. This value can be compared with a linear interpolation between bulk GaAs and InAs values using the gallium mole fraction $x = 0.4$ extracted above (from the fit to the PL and intersublevel energies), which gives $\gamma = 18$ au.

We find good overall agreement between the measured and calculated population recovery of the QD ground state. In particular, we are able to predict the increase of the weight of the long

⁸ An accurate determination of the low temperature long decay time component for sample B is not possible due to the limited delay stage scanning range (1.2 ns) and the value of ~ 5 ns we claim here is the lower limit.

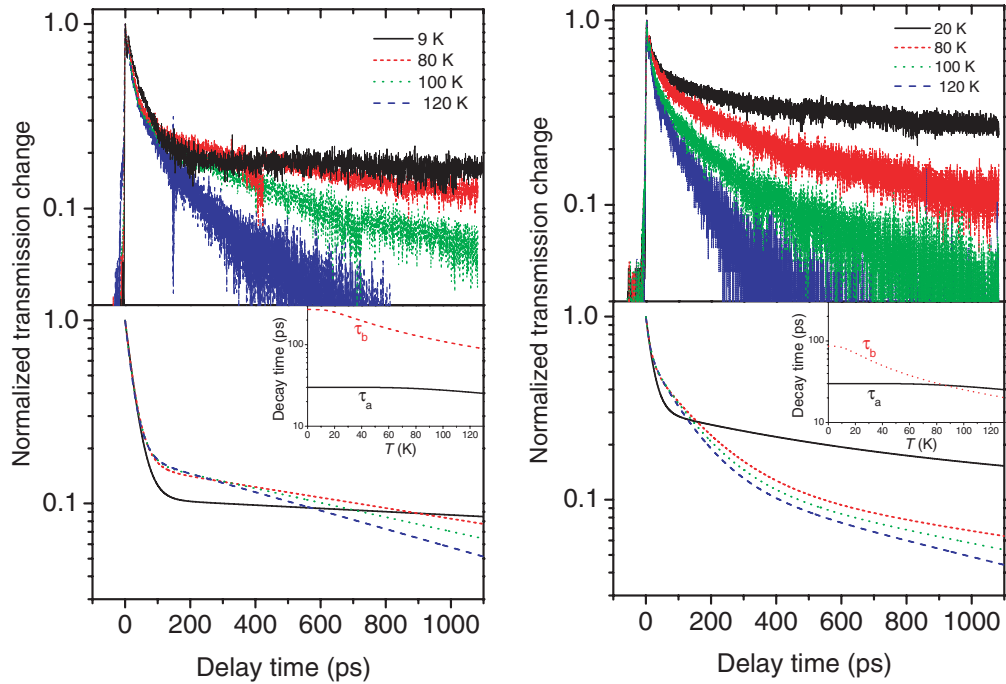


Figure 5. Measured and calculated temperature dependence of the pump–probe dynamics for two electron per dot samples B (a) and C (b). Insets: decay times τ_a (black solid line) and τ_b (dashed red line) plotted as a function of the temperature.

decay component when the anisotropic splitting increases. Let us remark that the short decay time is governed by τ_a and independent of V_A , while the relative initial (i.e. extrapolated to zero delay) amplitude of the long decay component is given by the ratio $\sim \tau_a/\tau_b$. As τ_a is equal in both samples, calculations predict a decrease of τ_b as the anisotropic splitting increases (see figure 3), thus increasing the weight of the long decay component. A slight discrepancy between the absolute value of long decay component observed experimentally and its calculation might be due to the strong dependence of τ_b with respect to $2(V_E - V_A)$, as shown in figure 3. The difference between the measured (~ 2 ns) and calculated (~ 5 ns) long decay time for sample C is probably due to the relatively strong temperature dependence of the long decay component for this sample as we discuss below.

In figure 5, we show measured and simulated temperature dependence of the pump–probe dynamics. The insets of figure 5 show the calculated temperature dependence of the decay times τ_a and τ_b . The mechanism of polaron decay (τ_a) by phonon anharmonicity is the disintegration into 2 acoustic phonons of equal energy (~ 27 meV), as extracted from previous measurements [25], which is rather insensitive to the temperature below 120 K. Therefore, when increasing the temperature, the main effect is to decrease the relaxation times τ_b and τ_c and their corresponding reverse decay times τ_b^- and τ_c^- by absorption of acoustic phonons (not shown in figure 2). As a consequence, the ratio τ_a/τ_b increases and thus the fractional contribution of long decay component is expected to increase. This effect is experimentally observed for sample B (see figure 5(a)) where an increase of the temperature from 20 to 80 K leads to an increase of the long decay time contribution. Additionally, the long decay time decreases as reverse processes involving absorption of acoustic phonons (times τ_c^- and τ_b^-) allow relaxation to the

ground state via the excited singlet state. There is a significant difference in the spin relaxation between these two samples, which is determined by the anisotropic splitting energy. Thus for sample B, after the spin flip occurs, the triplet polarons rapidly relax (with the characteristic transition time $\tau_c \sim 90$ ps) to the lower triplet state $|sp_x\rangle^T$. At low temperature, the long decay time observed is then governed by triplet state lifetime τ_e , while with increasing temperature the reverse processes τ_c^- and τ_b^- lead to a decrease of the triplet to singlet spin–flip time with the activation energy of $2V_E$. In contrast, for sample C, τ_c is considerably longer (~ 1 ns), because of the larger anisotropic splitting (see figure 3). As a consequence, for delay times below 500 ps polarons still mainly occupy the upper triplet state $|sp_y\rangle^T$. Triplet to singlet state spin–flip processes therefore occur mainly due to the re-absorption of the acoustic phonons (τ_b^-) with the characteristic energy of $2(V_E - V_A)$, which is only 3 meV for this sample. Consequently, the reverse triplet to excited singlet spin–flip is more easily thermally activated in sample C than in B. In figure 5, the predicted difference in the temperature dependence between these two samples is observed in experiments, further demonstrating the good agreement between our experimental results and the theory. Above 100 K, a more rapid decrease of the measured pump–probe signal compared with our simulations might be explained by the possible contribution of higher energy QD excited states, which are not included in our model.

4. Conclusion

In conclusion, we have investigated polaron relaxation in QDs containing 2 electrons using intraband pump–probe measurements. A reduction of the singlet polaron lifetime compared to the one-electron polaron is observed, as predicted by the enhancement of the Fröhlich coupling. Spin–flip transitions between singlet and triplet states are observed, in agreement with calculations based on Dresselhaus spin–orbit interactions and electron–phonon couplings. We have shown that the spin–flip time between excited singlet and triplet states depends strongly on the anisotropic splitting between the p -states. A spin triplet lifetime of ~ 5 ns is measured at low temperature. These results underline the importance of the spin–orbit coupling in the energy relaxation of QDs containing two or more electrons.

Acknowledgments

Funding was provided by the UK Engineering and Physical Sciences Research Council (EPSRC) under the EPSRC/FOM agreement, and grant numbers GR/S76076/01 and GR/T21158/01. The LPA (UMR 8551) is associated with the CNRS and the Universities Paris 6 and Paris 7. The free-electron laser ‘FELBE’ is supported by the Integrating Activity on Synchrotron and Free-Electron Laser Science (IA-SFS) under the EU contract RII3-CT-2004-506008 of the 6th Framework ‘Structuring the European Research Area, Research Infrastructures Action’. In addition, we would like to thank Professor D Whittaker for useful discussions and Dr B Redlich and the FELIX staff for their help and guidance.

Appendix. Triplet polaron calculation

We use the Huang–Rhys formalism in order to describe singlet and triplet polaron ground states. From annihilation and creation operators $a(q)$ and $a^+(q)$ of LO-phonon of wavevector q , new

annihilation and corresponding creation operators are defined by [26]:

$$b_{ss}(q) = a(q) + 2S_s(q), \quad (\text{A.1a})$$

$$b_{sp_x}(q) = a(q) + S_s(q) + S_{p_x}(q), \quad (\text{A.1b})$$

where $S_s(q)$ and $S_{p_x}(q)$ are defined by:

$$S_s(q) = \frac{\langle s, 0_q | H_F | s, 1_q \rangle}{E_{LO}}, \quad (\text{A.2a})$$

$$S_{p_x}(q) = \frac{\langle p_x, 0_q | H_F | p_x, 1_q \rangle}{E_{LO}}. \quad (\text{A.2b})$$

The fundamental modes corresponding to operators $b_{ss}(q)$ and $b_{sp_x}(q)$ are respectively $|\widetilde{0}_{ss}\rangle$ and $|\widetilde{0}_{sp_x}\rangle$. The new eigenstates are respectively the singlet polaron ground state $|ss, \widetilde{0}_{ss}\rangle$ and the triplet polaron state $|(sp_x)^T, \widetilde{0}_{sp_x}\rangle$. The one-phonon replicas of the singlet ground state read $|ss, \widetilde{1}_{ss}(q)\rangle$, where $|\widetilde{1}_{ss}(q)\rangle = b_{ss}^+(q)|\widetilde{0}_{ss}\rangle$.

In equation (9), mixing between triplet and singlet one-phonon replica involves the following vectorial products:

$$\langle \widetilde{0}_{sp} | \widetilde{0}_{ss} \rangle = \exp\left(-\frac{1}{2} \sum_q |S_s(q) - S_p(q)|^2\right), \quad (\text{A.3})$$

$$\langle \widetilde{0}_{sp} | \widetilde{1}_{ss}(q) \rangle = \langle \widetilde{0}_{sp} | b_{sp}^+(q) + S_s^*(q) - S_{p_x}^*(q) | \widetilde{0}_{ss} \rangle = [S_s^*(q) - S_{p_x}^*(q)] e^{-\frac{1}{2} \sum_q |S_s(q) - S_p(q)|^2}. \quad (\text{A.4})$$

Finally, in order to calculate the triplet polaron lifetime (equation (10)), we compute:

$$\sum_q |\langle \widetilde{0}_{sp} | \widetilde{1}_{ss}(q) \rangle|^2 = Y e^{-Y}, \quad (\text{A.5})$$

where $Y = \sum_q |S_s(q) - S_p(q)|^2$.

References

- [1] Inoshita T and Sakaki H 1992 *Phys. Rev. B* **46** 7260
- [2] Knipp P A, Reinecke T L, Lorke A, Fricke M and Petroff P M 1997 *Phys. Rev. B* **56** 1516
- [3] Hameau S, Guldner Y, Verzelen O, Ferreira R, Bastard G, Zeman J, Lemaître A and Gérard J-M 1999 *Phys. Rev. Lett.* **83** 4152
- [4] Hameau S, Isaia J N, Guldner Y, Deleporte E, Verzelen O, Ferreira R, Bastard G, Zeman J and Gerard J M 2002 *Phys. Rev. B* **65** 085316
- [5] Carpenter B A, Zibik E A, Sadowski M L, Wilson L R, Whittaker D M, Cockburn J W, Skolnick M S, Potemski M, Steer M J and Hopkinson M 2006 *Phys. Rev. B* **74** 161302(R)
- [6] Li X-Q, Nakayama H and Arakawa Y 1998 *Phys. Rev. B* **59** 5069
- [7] Verzelen O, Ferreira R and Bastard G 2000 *Phys. Rev. B* **62** R4809
- [8] Sauvage S, Boucaud P, Lobo R P S M, Bras F, Fishman G, Prazeres R, Glotin F, Ortega J M and Gérard J-M 2002 *Phys. Rev. Lett.* **88** 177402
- [9] Zibik E A *et al* 2004 *Phys. Rev. B* **70** 161305(R)
- [10] Kroutvar M, Ducommun Y, Heiss D, Bichler M, Schuh D, Abstreiter G and Finley J J 2004 *Nature* **432** 81

- [11] Cortez S, Krebs O, Laurent S, Senes M, Marie X, Voisin P, Ferreira R, Bastard G, Gérard J-M and Amand T 2002 *Phys. Rev. Lett.* **89** 207401
- [12] Findlay P C *et al* 1998 *Phys. Rev. B* **58** 12908
- [13] Zibik E A *et al* 2005 *Physica E* **26** 408
- [14] Nabetani Y, Ishikawa T, Noda S and Sakaki A 1994 *J. Appl. Phys.* **76** 347
- [15] Stier O, Grundmann M and Bimberg D 1999 *Phys. Rev. B* **59** 5688
- [16] Bester G, Nair S and Zunger A 2003 *Phys. Rev. B* **67** 161306(R)
- [17] Ediger M, Bester G, Gerardot B D, Badolato A, Petroff P M, Karrai K, Zunger A and Warburton R J 2007 *Phys. Rev. Lett.* **98** 036808
- [18] Isaia J N, de Vaulchier L A, Hameau S, Ferreira R, Guldner Y, Deleporte E, Zeman J, Thierry-Mieg V and Gerard J-M 2003 *Eur. Phys. J. B* **35** 209
- [19] Dresselhaus G 1955 *Phys. Rev.* **100** 580
- [20] Cardona M, Christensen N E and Fasol G 1988 *Phys. Rev. B* **38** 1806
- [21] Tackeuchi A, Wada O and Nishikawa Y 1997 *Appl. Phys. Lett.* **70** 1131
- [22] Bulaev D V and Loss D 2005 *Phys. Rev. B* **71** 205324
- [23] Braun P F *et al* 2005 *Phys. Rev. Lett.* **94** 116601
- [24] Grange T, Ferreira R and Bastard G unpublished
- [25] Zibik E A *et al* 2004 *Phys. Status Solidi c* **1** 2613
- [26] Huang K and Rhys A 1950 *Proc. R. Soc. Lond. A* **204** 406